Evaluation of MafG interaction with Maf recognition element arrays by surface plasmon resonance imaging technique

Motoki Kyo[1], Tae Yamamoto[2], Hozumi Motohashi[2], Terue Kamiya[1], Toshihiro Kuroita[1], Toshiyuki Tanaka[3], James Douglas Engel[4], Bunsei Kawakami[1] and Masayuki Yamamoto[2,4,5,*]

[1]*TOYOBO Co. Ltd. Bio 21 Project, 10-24 Toyo-Cho, Tsuruga, Fukui 914-0047, Japan*

[2]*Centre for Tsukuba Advanced Research Alliance, University of Tsukuba, 1-1-1 Tennodai, Tsukuba 305-8577, Japan*

[3]*Institute of Applied Biochemistry, University of Tsukuba, 1-1-1 Tennodai, Tsukuba 305-8572, Japan*

[4]*Cell and Developmental Biology, University of Michigan Medical School, Ann Arbor, MI 48109-0616, USA*

[5]*ERATO Environmental Response Project, Japan Science and Technology Corporation, 1-1-1 Tennodai, Tsukuba 305-8577, Japan*

Specific interactions between transcription factors and *cis*-acting DNA sequence motifs are primary events for the transcriptional regulation. Many regulatory elements appear to diverge from the most optimal recognition sequences. To evaluate affinities of a transcription factor to various suboptimal sequences, we have developed a new detection method based on the surface plasmon resonance (SPR) imaging technique. Transcription factor MafG and its recognition sequence MARE (*Maf r*ecognition *e*lements) were adopted to evaluate the new method. We modified DNA immobilization procedure on to the gold chip, so that a double-stranded DNA array was successfully fabricated. We further found that a hydrophilic flexible spacer composed of the poly (ethylene glycol) moiety between DNA and alkanethiol self-assembled monolayers on the surface is effective for preventing nonspecific adsorption and facilitating specific binding of MafG. Multiple interaction profiles between MafG and six of MARE-related sequences were observed by the SPR imaging technique. The kinetic values obtained by SPR imaging showed very good correlation with those obtained from electrophoretic gel mobility shift assays, although absolute values were deviated from each other. These results demonstrate that the double-stranded DNA array fabricated with the modified multistep procedure can be applied for the comprehensive analysis of the transcription factor-DNA interaction.

Introduction

Specific interactions between transcription factors and *cis*-acting DNA sequence motifs form the molecular basis of the gene expression regulation. Many preceding studies have revealed that one transcription factor usually binds to multiple related *cis*-acting motifs and, conversely, multiple related transcription factors bind to one *cis*-acting DNA motif. However, it has been very difficult technically to identify a specific and important interaction for each transcription factor and *cis*-acting motif. Detailed comparison of the binding affinities between transcription factors and specific *cis*-acting motifs therefore would provide important clue for our understanding of the transcription factor function.

The Maf family proteins appear to be typical members of a large group of regulatory factors characterized by a

basic region and leucine zipper (bZip) structure (Motohashi *et al.* 2002). The founding member of this family, v-Maf, is an oncogene, which was discovered as the transforming component of the avian musculoaponeurotic fibrosarcoma virus, AS42 (Nishizawa *et al.* 1989). Subsequently, it was found that the cellular homologue, from which v-Maf was originally transduced (c-Maf), was but one member of a multigene family of related transcription factors. To date, this family consists of four large Maf family members, c-Maf, MafB, NRL, and L-Maf / A-Maf, and three small Maf proteins, MafF, MafG, and MafK (Kataoka *et al.* 1994b, 1995; Swaroop *et al.* 1992; Ogino & Yasuda 1998; Fujiwara *et al.* 1993). The proteins interacting with the small Maf family members have been expanding to include new members in Cap'n'collar (CNC) and Bach families: p45 NF-E2, Nrf1 / LCR–F1, Nrf2/ECH, Nrf3, Bach1, and Bach2 (Andrews *et al.* 1993; Chan *et al.* 1993; Moi *et al.* 1994; Itoh *et al.* 1995; Kobayashi *et al.* 1999; Oyake *et al.* 1996). The superficially arbitrary division of the Maf

family into small and large members is likely of functional consequence, since all of the large Mafs appear to contain a recognizable transactivation domain, while the small Mafs encode slightly more than the DNA binding and dimerization motifs.

The bZip domain of the Maf factors are characterized by the presence of extended homology region (EHR), which is located in the N-terminal side of the basic region (Swaroop *et al.* 1992; ancillary DNA binding region, Kerppola & Curran 1994). DNA-binding specificity of the Maf family factors was determined by PCR–gel mobility shift assay (GMSA) amplification and purification method (Kerppola & Curran 1994; Kataoka *et al.* 1994a). Conclusion of these studies are that Maf factors recognize relatively long palindromic DNA sequences, TGCTGA^G/$_C$TCAGCA and TGCTGA^{GC}/$_{CG}$TCAGCA, which are now known as Maf recognition elements (MAREs). MAREs contain either TPA-responsive element (TRE; TGA^G/$_C$TCA) or cAMP-responsive element (CRE;TGA^{GC}/$_{CG}$TCA) as a core sequence, and extended elements on both sides of the core sequence (flanking region; 5′-TGC-core-GCA-3′). The recognition of the flanking region in MARE by EHR distinguishes the Maf family proteins from members of the AP-1 or CREB family of the bZip transcription factor superfamily. Kerppola & Curran (1994) showed evidence that the consensus sequence of large Maf binding is TGC(N)$_{6-7}$GCA. Since the flanking region of MARE is consistently required, the study strongly suggests an important contribution of the flanking region to the Maf-specific DNA-binding. Indeed, we showed that Maf EHR is important for the flanking region recognition (Kusunoki *et al.* 2002). It has also been reported through amino acid replacement/ mutation analysis that a unique amino acid in the basic region is involved in the flanking region recognition by Maf proteins (Dlakic *et al.* 2001).

Currently, GMSA is a standard method to examine the interaction between transcription factors and DNA motifs and to obtain an equilibrium constant. However, GMSA is a low-throughput method for quantification of the interaction, which usually requires labourious sample preparation steps. Recently, electrodes (Boon *et al.* 2002) and surface plasmon resonance (SPR, Jost *et al.* 1991; Suzuki *et al.* 1998) techniques have been developed, and these techniques are exploited to analyse the interaction between surface immobilized molecules and those in solution. Especially, SPR has advantages that it does not require any labelled reagents and can be applied for the wide surface area (Jordan & Corn 1997). The SPR technique is especially useful for a semiquantitative analysis, as it detects a dynamic real-time interaction profile.

Another recent progress has been made in the field of chip technology, which has been applied for the study of various interactions among proteins and nucleic acid fragments as microarrays (Schena *et al.* 1995; MacBeath & Schreiber 2000; Zhu *et al.* 2001; Bulyk *et al.* 2001; Newman & Keating 2003). Indeed, Nelson *et al.* (1999) developed a prototype of imaging technique for the detection of the biomolecular interaction by combining the SPR and chip technology. This SPR imaging technique seems to enable us to analyse multiple protein–DNA interactions simultaneously and comprehensively. In this respect, SPR is more advantageous than the methods exploiting electrodes upon combination with the chip technology for a comprehensive analysis, since it would be very labourious to construct an array of tiny electrodes on a chip.

Although a multistep array fabrication procedure has been developed for the SPR-chip imaging to detect the protein–DNA interactions (Brockman *et al.* 1999), application of this technology has been hampered due to technical difficulties. In particular, double-stranded DNAs could not be directly immobilized on the chip surface, as organic solvent used in the original procedure easily denatures delicate biomolecules. In the previous procedure (Brockman *et al.* 1999), single-stranded oligonucleotides were first attached on to the gold surface followed by the hybridization with the complementary DNAs to generate double-stranded DNAs on the chip. However, in order to perform a comprehensive affinity quantification of transcription factors to various suboptimal sequences, it is required to fabricate a double-stranded DNA array composed of multiple sequences that are very similar to one another. Immobilization of preannealed double-stranded DNAs is highly preferable for preventing mismatched hybridization and for assuring complete pairing between complementary DNAs.

To develop an efficient and reliable method to detect specific protein–DNA interactions exploiting the SPR technology, we have designed in this study a modified multistep procedure for generation of DNA array on the gold surface, which does not require steps exposing DNA to noxious organic solvents. We also found a better heterobifunctional crosslinker that reduces nonspecific adsorption of the protein to the chip surface in the immobilization process. By utilizing the SPR imaging technique with the newly developed double-stranded DNA array, we then examined binding affinity of MafG, one of the small Maf family members, to several MARE-related DNA sequences. The relative affinities between MafG, various MARE-related sequences showed a very good correlation to those obtained from GMSA. Thus, the new surface immobilization procedure has enabled various delicate biomolecules, including double-stranded

DNAs, to be attached stably on to the gold chip in their native form. This procedure provides a solid basis for the study of SPR-based protein-DNA interactions.

Results

Procedure for immobilization of biomolecules on gold surface

A seven-step fabrication procedure has been used for the immobilization of biomolecules on the gold surface (Brockman *et al*. 1999), which was based on self-assembled monolayers (SAMs) of alkanethiol (Troughton *et al*. 1988; Chidsey & Loiacono 1990) and photolithography technique (Tarlov *et al*. 1993; Huang *et al*. 1994). In the procedure, the hydrophobic protecting group, 9-Fluorenylmethoxycarbonyl (Fmoc), was used for the background protection, and it was deprotected by weak base in organic solvent after single-stranded DNA was immo-

bilized on the surface. In the final step of this procedure, an N-hydroxysuccinimido ester poly(ethylene glycol) (NHS-PEG) was reacted to an amino group on the surface. In these processes, the immobilized single-stranded DNAs were exposed to organic solvents and NHS-PEG.

In order to avoid exposure of test biomolecules to noxious effect, we established a modified procedure to fabricate double-stranded DNA array on the gold surface using thiol-terminated methoxypoly(ethylene glycol), PEG-thiol. This procedure consists of 5 steps described in Fig. 1. Step 1 is the PEG-thiol immobilization on the whole surface area of a gold slide; Step 2 is the photo-patterning by UV irradiation shielded with a bored chromium quartz mask; Step 3 is the introduction of amine terminated alkanethiol on the irradiated spots; Step 4 is the creation of maleimido surface on the spots by reacting with a hetero-bifunctional crosslinker, which contains a NHS ester and a maleimido group; Step 5 is the 5′-thiol-terminated DNA immobilization by thiol-maleimido coupling reaction.
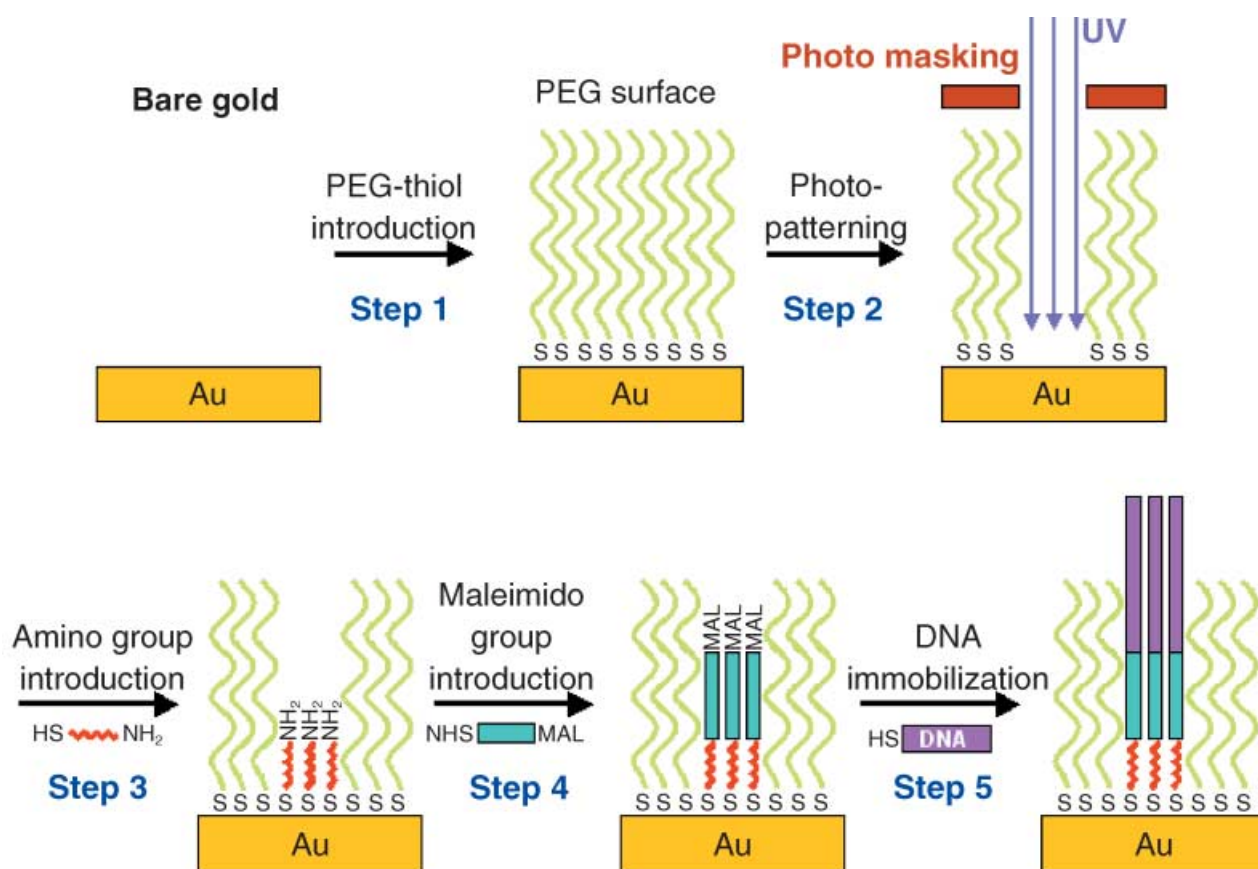

Figure 1 The scheme of surface chemistry to immobilize 5′-thiol terminated DNA. Five steps of DNA immobilization procedure are illustrated. The hydrophilic polymer, PEG-thiol, is first immobilized, which serves as the background of the array (Step 1). DNA spots are created by modifying a self-assembled monolayer of amine terminated alkanethiol, 8-AOT (Steps 2 and 3), with a heterobifunctional crosslinker to prepare a maleimido surface (Step 4). 5′-thiol terminated DNA is added to the spotted region (Step 5).
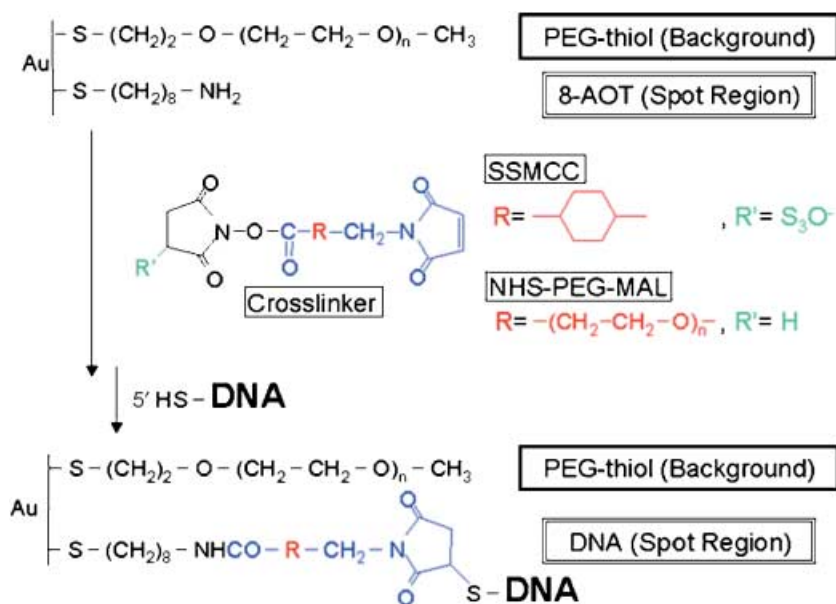
Figure 2 Two different heterobifunctional crosslinkers for specific binding of MafG to DNA array. Two heterobifunctional crosslinkers sulfosuccinimidyl-4-(*N*-maleimidomethyl)cyclohexane-1-carboxalate (SSMCC) and *N*-hydroxysuccinimide-PEG maleimido MW 3400 (NHS-PEG-MAL), were tested for the immobilization of 5′-thiol modified oligonucleotides. SSMCC provides a hydrophobic short linker, while NHS-PEG-MAL possesses a hydrophilic and flexible spacer region.

During these processes, DNA was not exposed to any organic solvents and reagents, since the DNA immobilization was the final step for the array fabrication. Therefore, this modification enabled us to fabricate an array of delicate molecules, such as double-stranded DNAs.

Heterogeneous PEG crosslinker for specific binding of MafG to DNA array

In our effort to establish a standard method for fabrication of a double-stranded DNA array, we also examined the usage of heterobifunctional crosslinkers. Two hetero-bifunctional crosslinkers, sulfosuccinimidyl-4-(*N*-maleimidomethyl)cyclohexane-1-carboxalate (SSMCC) and *N*-hydroxysuccinimide-PEG maleimido MW 3400 (NHS-PEG-MAL), were tested for the immobilization of 5′-thiol modified oligonucleotides (Fig. 2). SSMCC

provides a hydrophobic short linker, while NHS-PEG-MAL possesses a hydrophilic and flexible spacer region.

In comparing the two above-mentioned crosslinkers, we first adopted the sequential DNA immobilization method to assure the generation of double-stranded DNAs on the surface. The reaction scheme to attach DNA on to the chip surface is shown in Fig. 2. 5′-thiol-terminated single-stranded oligonucleotides were first reacted with the maleimido moiety provided by either SSMCC or NHS-PEG-MAL, and the complementary oligonucleotides were hybridized to generate double-stranded DNAs on the surface. Two of MARE-related sequences, MARE25 and MARE23 (Kataoka *et al.* 1994a), were chosen for the assay (Table 1). MARE25 sequence completely matches the consensus sequence for the MafG homodimer binding, while MARE23 sequence has a conserved core region with the altered flanking region.

Table 1 MARE-related sequences for surface immobilization

	5′											3′
MARE25	T	G	C	T	G	A	C	T	C	A	G	C	A
hOPSIN	T	G	C	T	G	A	**T**	T	C	A	G	C	**C**
hNQO1m	**A**	G	**T**	T	G	A	C	T	C	A	G	C	A
MARE23	**C**	**A**	**A**	T	G	A	C	T	C	A	**T**	**T**	**G**
hBglHS4	**G**	G	C	T	G	A	C	T	C	A	**C**	**T**	**C**
mGSTY	T	G	**G**	T	G	A	C	**A**	**A**	A	G	C	A

The bases different from the MARE25 sequence are in bold. MARE25 contains binding motif that matches the consensus sequence for TRE-type MARE, while MARE23 sequence has a conserved core region with altered flanking region. Flanking sequence of hNQO1 MARE was modified to make the crucial G to be conserved. For this reason we named the DNA as hNQO1m.

Previous GMSA showed that MafG homodimer strongly binds to MARE25, but scarcely to MARE23, suggesting that the flanking sequence of MARE is critical for DNA binding of Maf family proteins (Kataoka *et al*. 1995).

A single-stranded DNA array with the two sequences, MARE25 and MARE23, was fabricated and sequentially exposed to 1 μM of their complementary oligonucleotides and 125 nM of MafG homodimer. Figure 3A,B show binding profiles simultaneously observed at three test spots, MARE25, MARE23 and blank (a spot with free maleimido groups), as well as one background area (a spot with free PEG-thiol groups) by SPR imaging technique. The increases of SPR signals by the addition of the complementary oligonucleotides were detected in both spots of MARE25 and MARE23, which suggests the

generation of double stranded DNAs by hybridization. Importantly, no cross-hybridization was observed in these processes, indicating that the arrays were fabricated properly without base mis-pairing. When MafG was applied to the flow on the SSMCC-immobilized array, the SPR signals were increased marginally at both MARE25 and MARE23 spots, which indicates that MafG did not interact efficiently with both DNAs under this condition (Fig. 3A). On the contrary, a robust increase of SPR signal was observed for MARE25, but not for MARE23, on the NHS-PEG-MAL-immobilized array (Fig. 3B). The results were in very good agreement with the previous GMSA results, demonstrating that specific DNA-binding of MafG homodimer was reproduced on the NHS-PEG-MAL-immobilized array, but not on the SSMCC-immobilized array. Therefore, the NHS-PEG-MAL was chosen in this study for the analysis of interaction between MafG and MARE-related sequences.

Salt concentration affects kinetic SPR measurements

Among various components of the SPR binding buffer, we found that the salt concentration had the greatest influence on the occurrence of nonspecific binding of transcription factors. We measured the SPR signals after continuous MafG application for 30 min at different sodium chloride concentrations from 150 mM to 300 mM (Table 2). When the sodium chloride concentration is 150 mM or less, the nonspecific binding was observed at the blank spot and PEG background on the chip, judged from the smaller value of S_1/N ratio (Table 2 and data not shown). In contrast, when 300 mM sodium chloride was applied, S_1 value (Table 2) became low, suggesting that the specific binding was inhibited. We therefore utilized intermediate concentration of sodium chloride, i.e. 200 mM, for the MafG analysis.

Under the final binding condition (20 mM HEPES-HCl (pH 7.9), 200 mM NaCl, 4 mM MgCl$_2$, 1 mM EDTA, and 100 μg/ml BSA), MafG sufficiently bound to MARE25, but not MARE23, and the kinetic data were obtained for MARE25 as k_a (association rate constant) $= 4.11 \times 10^4$ (M^{-1} s^{-1}), k_d (dissociation rate constant) $= 1.49 \times 10^{-4}$ (s^{-1}), and K_D (dissociation constant) $= 3.63 \times 10^{-9}$ (M) by curve fitting calculation from simple binding model (George *et al*. 1995).

Interaction between MafG and MARE-related sequences examined on one chip

We then evaluated a double-stranded DNA array fabricated by the new immobilization method. Each pair of complementary oligonucleotides was first annealed
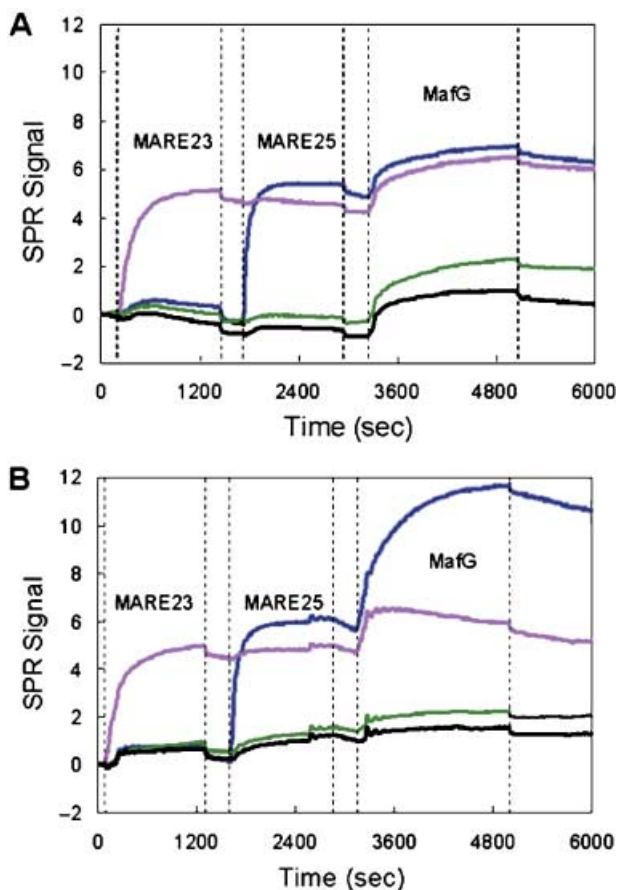

Figure 3 Sequential DNA immobilization method for generation of double-stranded DNAs on chip surface. The SPR signal changes by the exposure to 1 μM of complementary oligonucleotides of MARE25 and MARE23, and subsequently to 125 nM of MafG homodimer. The changes are monitored at MARE25 (blue), MARE23 (purple), blank (green), and background (black). Single-strand DNA was immobilized on the surface via (A) SSMCC and (B) NHS-PEG-MAL.

M Kyo *et al.*

Table 2 Influence of salt concentration on SPR signals

NaCl concentration	SPR signal			S_1/S_2	S_1/N
	MARE25 (S_1†)	MARE23 (S_2†)	Background (N†)		
150 mM	13.40 ± 1.70	6.60 ± 0.85	5.44 ± 0.56	2.04	2.47
200 mM	20.00 ± 3.90	4.57 ± 1.83	1.24 ± 0.02	4.38	16.10
300 mM	8.07 ± 2.49	1.24 ± 0.21	1.80 ± 1.78	6.51	4.50

†SPR signals obtained after continuous MafG application for 30 min. S_1, S_2 and N are the values at the spots of MARE25, MARE23 and the background area, respectively.

and then immobilized on the surface of a gold chip. The double-stranded oligonucleotides were spotted by an automated spotter and immobilized through the thiol-modified 5′-protruding end on the gold surface via NHS-PEG-MAL. We chose four MARE-related sequences found in the regulatory regions of four endogenous genes (Table 1), including human NQO1 (hNQO1m MARE; Venugopal & Jaiswal 1996), mouse GSTy (mGSTY MARE; Itoh *et al.* 1997), human β-globin gene (hBglHS4 MARE; Stamatoyannopoulos *et al.* 1995), and human rhodopsin gene (hOPSIN MARE; Kumar *et al.* 1996). The importance of these MAREs has been examined functionally in co-transfection-transactivation analyses. The human NQO1 MARE has an altered flanking region on one side, which is similar to human β-globin MARE. To examine MAREs encompassing various categories, we modified flanking sequence of human NQO1 MARE so that the crucial 'G' in the flanking region is conserved symmetrically (Table 1). For this reason, we named the DNA as hNQO1m. In addition to these MAREs, both MARE25 and MARE23 were spotted as a positive and negative control, respectively.

The chip with the immobilized double-stranded DNAs was placed to the SPR imaging instrument, and 125 nM of MafG homodimer was applied for the DNA-protein association analysis. The SPR signal profiles of association and dissociation were observed for 1800 s with MafG-containing buffer and for the following 1200 s with the blank buffer, respectively. These results are shown in the conventional binding curves in Fig. 4A. To visualize the results more effectively, we also calculated the signals utilizing Scion Image software and the results are shown in the form of SPR difference image in Fig. 4B. The association and dissociation rate constants were calculated from the curve profiles (Fig. 4, *n* = 3) and summarized in Table 3. Although k_a and k_d values obtained from the single-stranded DNA array were slightly lower than those obtained from the double-stranded array, K_D values of MARE25 were almost the same in the two distinct
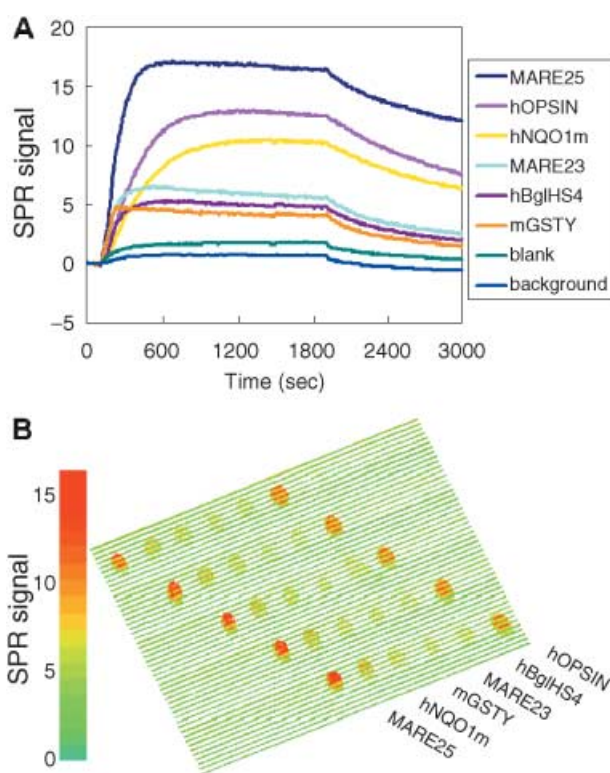

Figure 4 Interaction between MafG and MARE-related sequences examined on one chip with a double-stranded DNA array. (A) The SPR signal changes by the exposure to 125 nM MafG homodimer on the double-stranded DNA array where six MARE-like sequences are immobilized. The buffer with MafG started to flow at 0 s and was terminated at time 1800 s. The buffer without MafG was replaced and continued for the following 1200 s. Representative binding curves, each of which was obtained from a single spot, are shown. Three independent experiments were performed, and the kinetic data were calculated (see Table 3). (B) SPR difference image showing the binding of the MafG homodimer on to the double-stranded DNA array after the exposure to 125 nM MafG. Five independent spots of each oligonucleotide were generated for visualizing a representative image.

Table 3 Kinetic values of interactions between MafG homodimer and MARE-related sequences calculated from SPR profiles and GMSA

	SPR average			GMSA
	k_a [M^{-1} s^{-1}] 10^5	k_d [s^{-1}] 10^{-4}	K_D [M] 10^{-9}	K_D [M] 10^{-7}
MARE25	1.36 ± 0.32	3.13 ± 0.66	2.50 ± 1.02	2.49 ± 0.06
hOPSIN	0.50 ± 0.06	3.72 ± 0.30	7.68 ± 1.17	2.52 ± 0.05
hNQO1m	0.39 ± 0.04	3.24 ± 0.36	8.59 ± 1.75	2.73 ± 0.13
mGSTY	ND	ND	ND	ND
MARE23	ND	ND	ND	ND
hBglHS4	ND	ND	ND	ND

SPR was measured 3 times, and the average and standard deviation are shown. ND not able to determine. k_a, association rate constant; k_d, dissociation rate constant; K_D, dissociation constant.

arrays (see above and Fig. 3B). A reason for the difference in k_a and k_d values is unknown, but the similar K_D values suggest that the double-stranded DNA was properly immobilized on the surface without being denatured. The SPR difference image (Fig. 4B) was calculated from the SPR signals before and after exposure to MafG, and these signals represent that MafG properly binds to the spots. We interpret that MafG binds to MAREs specifically, since the signals on PEG background and a blank spot, where NHS-PEG-MAL is immobilized, are negligible. These results thus demonstrate successful establishment of a modified surface immobilization procedure for a double-stranded DNA array fabrication.

Kinetic data were calculated for the sequences to which substantial MafG binding was observed. Since MafG binds to DNA exclusively through forming a homodimer, it seems quite likely that observed kinetic data represent the interaction between MafG homodimer and double-stranded oligonucleotide containing MARE-related sequences. Of the six MARE and related sequences, sufficient amount of MafG interacted with MARE25, hOPSIN MARE, and hNQO1m MARE (Fig. 4). MARE25 displayed the highest affinity, and hOPSIN and hNQO1m MAREs are the next (Table 3). hOPSIN MARE has two base replacements in the MARE consensus sequence of MARE25; one is in the centre of the core region and the other is in the end of the flanking region. On the contrary, hNQO1m MARE possesses well conserved core region with mutated flanking region on one side (except that crucial G nucleotide was conserved). These observations suggest that the central bases and certain flanking bases of one side of MARE can be altered without affecting much the binding affinity to MafG. Interestingly, k_d are almost the same for MARE25, hOPSIN and hNQO1m MAREs, so the differences in K_D values should be attributable solely to those in k_a. On the other hand, MafG only weakly bound to mGSTY MARE, hBglHS4 MARE or MARE23. The results of hBglHS4 MARE and MARE23 indicate that mutations in both flanking regions eliminated the binding of MafG. Inability of mGSTY MARE to bind MafG implies that simultaneous mutations on one side of flanking region and the other side of core region may also inhibit the binding of MafG homodimer to MARE.

Comparison of K_D values obtained from SPR imaging technique and from GMSA

In order to evaluate validity of the SPR imaging technique, the K_D values obtained from the SPR binding analyses were compared to those from GMSA. The K_D values determined by GMSA for MARE25, hOPSIN MARE and hNQO1m MARE were ranged in the magnitude of 10^{-7} (Fig. 5, lanes 1–7 and 15–28). MARE25, hOPSIN MARE and hNQO1m MARE showed high affinities, and the highest was MARE25. On the contrary, weak MafG binding to mGSTY MARE was observed, albeit it was not enough for the K_D value determination (Fig. 5, lanes 29–35). No shifted bands were observed for MARE23 and hBglHS4 MARE (Fig. 5, lanes 8–14 and 36–42, respectively). These results are summarized in Table 3. Although K_D values calculated from the SPR signals are ranged in the magnitude of 10^{-9}, which are much smaller than those determined by GMSA, the comparative affinities obtained from these two distinct methods were very similar to each other. The affinity of MafG to MARE25 is the highest, and those to hOPSIN MARE and to hNQO1m MARE are intermediate. Interactions between MafG and mGSTY MARE, hBglHS4 MARE and MARE23 are not strong enough for the calculation of kinetic values.

Discussion

In this study, we have developed an improved surface chemistry suitable for the SPR-based interaction study
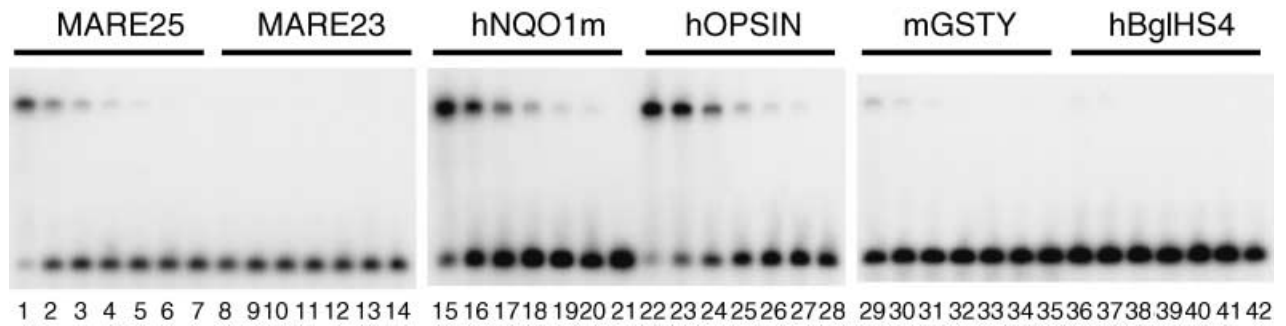
Figure 5 Interaction between MafG and MARE-related sequences observed in GMSA. Six different probes were used for GMSA, MARE25 (lanes 1–7), MARE23 (lanes 8–14), hNQO1m (lanes 15–21), hOPSIN (lanes 22–28), mGSTY (lanes 29–35) and hBglHS4 (lanes 36–42). MafG homodimer concentrations are 360 nM (lanes 1, 8, 15, 22, 29, 36), 180 nM (lanes 2, 9, 16, 23, 30, 37), 90 nM (lanes 3, 10, 17, 24, 31, 38), 45 nM (lanes 4, 11, 18, 25, 32, 39), 22.5 nM (lanes 5, 12, 19, 26, 33, 40), 11.3 nM (lanes 6, 13, 20, 27, 34, 41) and 0 nM (lanes 7, 14, 21, 28, 35, 42).

of biomolecules on the chip. In order to overcome an inconvenience that immobilized DNAs are easily denatured upon exposure to organic solvent and reactive PEG, we first constructed the background by using PEG-thiol, and test molecules were attached on to the spots in the final step. This procedure allowed pre-annealed double-stranded DNAs to be immobilized on the chip in native form. Exploiting this procedure, we successfully fabricated a double-stranded DNA array on the chip. An SPR imaging analysis based on this procedure was performed to examine the specific interaction between MafG and several MARE-related motifs. The SPR imaging analyses gave the consistent results with those obtained from GMSA as far as the relative affinities are concerned, which in turn support our contention that the detected SPR signals reflect specific binding of MafG to MAREs. Thus, this study demonstrates that the double-stranded DNA array fabricated with the modified multistep procedure can be applied for the comprehensive analysis of the transcription factor-DNA interaction.

In the classic SPR studies on the DNA-protein interaction, biotin-streptavidin chemistry was usually adopted (Seimiya & Kurosawa 1996; Galio *et al.* 1997; Suzuki *et al.* 1998; Oda *et al.* 1999). In this case, biotin-terminated oligonucleotides are usually attached on streptavidin-modified surface. This method, however, has an inherent problem upon applying for the array fabrication, as cross-contamination among the spots may happen due to a strong and quick binding reaction between biotin and streptavidin. In order to perform a comprehensive quantification of binding affinities of transcription factors to various suboptimal sequences, it is a prerequisite to fabricate a double-stranded DNA array composed of multiple sequences that are very similar

to one another. To this end, we adopted a method that allows immobilization of pre-annealed double-stranded DNAs on the chip, which can prevent mismatched hybridization and attain complete pairing between complementary DNAs. Indeed, we proved in this study that correct DNA immobilization was accomplished without contaminating spots in this procedure.

Another contrivance in this procedure is the choice of NHS-PEG-MAL as a heterobifunctional crosslinker. It should be noted that the interaction profiles between MafG and MAREs obtained with NHS-PEG-MAL-immobilized array show high level consistency with those observed in GMSA. This is in stark contrast to the results with SSMCC-immobilized array, as the latter results were not consistent with the GMSA data at all. We speculate that the flexible and hydrophilic linker provided by NHS-PEG-MAL might facilitate specific binding and prevent nonspecific adsorption of MafG by allowing the higher DNA mobility. We suppose that the PEG spacer should be generally effective to avoid nonspecific interactions of a test protein to the spot background regions. On the contrary, the salt concentration required for suppression of nonspecific binding must be determined for each protein.

Interactions between transcription factors and DNAs have been investigated by several methods including GMSA (Affolter *et al.* 1990; Yamamoto *et al.* 1990), filter-binding assay (Tanikawa *et al.* 1993) and SPR (Seimiya & Kurosawa 1996; Galio *et al.* 1997; Oda *et al.* 1999). The K_D values, determined by these methods, are ranging from 10^{-7} to 10^{-10} and, especially, those obtained by SPR are from 10^{-7} to 10^{-9}. One report compared K_D values calculated by GMSA and SPR, and showed that the values are almost similar to one another ranged in the magnitude of 10^{-9} (Suzuki *et al.* 1998). In our case, K_D

values obtained by SPR ranged around 10^{-9}, while those obtained by GMSA ranged around 10^{-7} (see Table 3). While the reason for this discrepancy is unclear at present, the following two differences in the measurement conditions may be pertinent.

First, DNA mobility is different from each other in the two measurements. Whereas DNAs are immobilized on a surface for SPR analysis, they are free in the solution in GMSA. Second, optimal salt concentrations are different from each other. Buffers with higher salt concentrations (more than 150 mM) are required for the SPR measurement to avoid the nonspecific adsorption of proteins on to the chip surface or immobilized DNA. On the contrary, GMSA buffer usually contains salts less than 75 mM, and nonspecific competitor DNA is typically added to the binding reaction solutions. In fact, we utilized in this study a high salt concentration (200 mM) to suppress nonspecific binding of DNA and MafG in the SPR analysis, whereas nonspecific DNA competitor was used for this purpose in GMSA. The kinetic profiles in the SPR measurement were investigated at various salt concentrations (Seimiya & Kurosawa 1996; Oda *et al.* 1999), and it was found that the lower salt concentration gives rise to the smaller k_d values, and that k_a values are usually not affected by the salt concentration. Consistent with the finding, we found that the dissociation of MafG and MARE25 became faster when sodium chloride concentration was as high as 450 mM (data not shown). Although these results do not explain the K_D value difference between SPR and GMSA, we still consider that both SPR and GMSA measurements are valid for quantitative interaction analysis, since there is a very good correlation between the K_D values of several MAREs obtained by SPR and GMSA.

All three small Maf family proteins are known to form either homodimer or heterodimer with other bZip superfamily members, including the CNC and Bach family members, and bind to MARE (Motohashi *et al.* 2002). These partner molecules cannot bind to MARE as a monomer or homodimer, so that small Mafs confer the DNA-binding ability on partner proteins and enable them to execute various activities directed by their functional domains through the heterodimerization. Since many of these Maf-based dimers exist in cells simultaneously, it seems very difficult to identify the primary Maf molecule or to evaluate the contribution of each dimer molecule to the gene regulation through a specific MARE in the regulatory region. One simple hypothesis is to assume that the most abundant dimer molecule in the nuclei may bind dominantly to MAREs, which leads to the notion that the balance between positive and negative regulators interacting to MAREs determines

the eventual transcriptional activity. In fact, by adopting megakaryocytic gene regulation directed by NF-E2 p45 and small Maf proteins, we showed that quantitative alteration enables small Maf proteins to direct both active and repressive transcription (Motohashi *et al.* 2000). In the absence of small Mafs, p45 does not bind to DNA, so MARE-dependent transcription cannot be activated. In the excess of small Mafs, transcriptionally inactive small Maf homodimer occupies MAREs and represses the transcription. Only at the optimal concentration of p45 and small Maf, the maximum level of transcriptional activation is achieved by p45/small Maf heterodimer.

Recent data suggest that the qualitative difference may also be important for the interaction of MAREs and Maf-based dimers. When we examined *mafG::mafK* compound null mutant mice, mutant animals displayed quite selective MARE-dependent transcriptional abnormality (Katsuoka *et al.* 2003). In the mice, heme oxygenase-1 (HO-1) mRNA level was markedly increased. Similarly, Bach1-null mutant mice exhibit selective increase of HO-1 mRNA level (Sun *et al.* 2002). However, no apparent influence of small Maf decrease is observed for other MARE-dependent genes (our unpublished observation), indicating that small Maf and Bach1 make a major contribution to HO-1 gene regulation.

Considering this situation, comprehensive evaluations become crucial for Maf-based dimer interactions with various MARE-related sequences. In this regard, quite recently the interactions between various bZip superfamily proteins were investigated *in silico* with glass slide-based protein arrays and fluorescent-labelled protein probes (Newman & Keating 2003). We analysed in this study the DNA-protein interaction. Our system enables to examine all possible variations in MAREs quantitatively by using a couple of gold chips or more, since simultaneous detection of 96 samples is technically feasible on one chip. We adopted MafG homodimer as our initial trial of this SPR-array technology, since it is the simple system composed of a single molecule. Obviously, next important analysis will be comparing binding profiles of MafG homodimer, Bach1/small Maf heterodimer, and the other Maf-based heterodimer molecules on one chip. We surmise that Bach1/small Maf heterodimer may have the strongest preference toward HO-1 MAREs.

In spite of discrepancy in absolute K_D values calculated from SPR and GMSA, there is a very good correlation between the two results in general. Since the SPR imaging is a powerful technique for the large-scale high-throughput analysis, we propose that the SPR imaging technique would be suitable for examining the general

binding preference of a transcription factor. We also propose that each specific interaction should be evaluated with the combination of multiple strategies, including SPR and GMSA for *in vitro* binding and reporter gene assay for *in vivo* binding.

Experimental procedures

Materials

The chemicals 8-amino-1-octanethiol, hydrochloride (8-AOT, Dojindo Laboratories), thiol terminated methoxypoly(ethylene glycol) MW 5000 (PEG-thiol, NOF), sulfosuccinimidyl-4-(*N*-maleimidomethyl)cyclohexane-1-carboxalate (SSMCC, Pierce), and *N*-hydroxysuccinimide-PEG maleimido MW 3400 (NHS-PEG-MAL, Shearwater), were all used as received.

Preparation of oligonucleotide DNAs

The oligonucleotides for covalent immobilization on the surface were designed as 5′-HS-(T)$_{15}$-CGGAAT(N)$_{13}$TTACTC-3′, and synthesized at Hokkaido System Science or Sigma Genosys with the thiol group protected. The 15-base thymine stretch with a thiol group on the 5′-end was added to the test sequence, which is composed of 13 variable sequence flanked by 6 fixed bases on both sides. 5′- and 3′-fixed sequences were CGGAAT and TTACTC, respectively. Table 1 outlines the various sequences we used in this study. The thiol group on the 5′-end of the oligonucleotides were deprotected, and they were purified by gel filtration with NAP-5 Columns (Amersham Biosciences) as described by Sigma Genosys. The complementary oligonucleotides were synthesized against the variable region with 6-base fixed regions on both sides. The double-stranded DNAs were prepared by annealing longer and shorter complementary DNAs with and without 5′-thiol group, respectively. 25 μM of 5′-thiolated strand and 100 μM of its complementary strand were annealed in the 5× SSC solution (75 mM sodium citrate, 750 mM NaCl; pH 7.0). The solution was heated to 94 °C for 5 min, and quenched to 4 °C for 15 min, then incubated at 37 °C for 3 h, to complete the annealing.

MafG protein preparation

MafG containing EHR and bZip motif, but lacking C-terminal 39 amino acids, was expressed in *Escherichia coli* as a His$_6$-tagged protein. The crude bacterial lysate was sequentially purified with SP sepharose (Pharmacia) and ProBond resin (Invitrogen). The recombinant protein was then cleaved with thrombin (Calbiochem) and further purified using SP sepharose. 200 μL of 125 nM MafG homodimer solution was used in one experiment.

Fabrication of DNA arrays

The covalently immobilized DNA array with PEG background was obtained by the following procedure. Gold layer (45 nm) with thin chromium underlayer (3 nm) on SF10 glass slide (Schott) were used for SPR imaging measurement. The gold slide was immersed in a PEG-thiol solution (1 mM in 1 : 6 H$_2$O: Ethanol) for at least 3 h to form PEG layer on the surface. This slide was patterned at 40 mW/cm^2 for 2 h with chromium quartz mask, which had 96 square holes of 500 μm, by UV light source, which was generated from a 500 W super high-pressure mercury lamp (Ushio, Tokyo). After the surface was rinsed with water and ethanol, the slide was soaked in 1 mM ethanolic solution of 8-AOT for 1 h. This resulted in 96 amino-functionalized 500 μm squares with PEG background. Thiol-reactive maleimido-modified surface was created with 1 mM solution of heterobifunctional crosslinker SSMCC or NHS-PEG-MAL in phosphate buffer (20 mM phosphate; pH 7.0 and 100 mM NaCl). 10 nL drop of 10 μM 5′-thiol-terminated DNA in phosphate buffer was delivered automatically on the patterned surface by using an automated spotter (Toyobo, Osaka), and the reaction was carried out for overnight. Then the surface was rinsed with phosphate buffer and 5× SSC solution containing 0.1% SDS.

SPR imaging analysis

The DNA array was placed immediately in the SPR imaging instrument (Toyobo). The SPR signals were obtained in the SPR buffer (20 mM HEPES (pH 7.9), 200 mM NaCl, 4 mM MgCl$_2$, 1 mM EDTA, and 100 μg/mL BSA). The SPR buffer and the sample in the same buffer were applied to the array surface with 100 μl/min. The SPR image and signal data were collected with MultiSPRinter Analysis program (Toyobo). The SPR difference image was constructed by using Scion Image (Scion, MD USA). The kinetic values were calculated with the program based on the simple reversible reaction model (George *et al.* 1995).

Gel mobility shift assays

Gel mobility shift assays were performed as previously described (Kataoka *et al.* 1994a). The same oligonucleotides with those used in SPR detection, which are composed of a 13 bp-variable sequence flanked by 6 bp-fixed regions on both sides, were end labelled with γ-^{32}P-ATP for generating probes. MafG protein was incubated with probes in the gel shift buffer (20 mM HEPES (pH 7.9), 20 mM KCl, 5 mM dithiothreitol, 4 mM MgCl$_2$, 1 mM EDTA, 100 μg/mL BSA and 400 μg/mL poly(dIdC)) at 37 °C for 30 min. The resulting mixture was subjected to native polyacrylamide gel electrophoresis and visualized by autoradiography. The K_D values were determined as described (Azam & Ishihama 1999) on the basis of the results obtained using protein concentration from 0 to 360 μM.

References

Affolter, M., Percival-Smith, A., Muller, M., Leupin, W. & Gehring, W.J. (1990) DNA binding properties of the purified Antennapedia homeodomain. *Proc. Natl. Acad. Sci. USA* **87**, 4093–4097.

Andrews, N.C., Erdjument-Bromage, H., Davidson, M.B., Tempst, P. & Orkin, S.H. (1993) Erythroid transcription factor NF-E2 is a haematopoietic-specific basic-leucine zipper protein. *Nature* **362**, 722–728.

Azam, T.A. & Ishihama, A. (1999) Twelve species of the nucleoid-associated protein from *Escherichia coli*. Sequence recognition specificity and DNA binding affinity. *J. Biol. Chem.* **274**, 33105–33113.

Boon, E.M., Salas, J.E. & Barton, J.K. (2002) An electrical probe of protein–DNA interactions on DNA-modified surfaces. *Nature Biotechn.* **20**, 282–286.

Brockman, J.M., Fruto, A.G. & Corn, R.M. (1999) A multi-step chemical modification procedure to create DNA arrays on gold surfaces for the study of protein–DNA interaction with surface plasmon resonance imaging. *J. Am. Chem. Soc.* **121**, 8044–8051.

Bulyk, M.L., Huang, X., Choo, Y. & Church, G.M. (2001) Exploring the DNA binding specificities of zinc fingers with DNA microarrays. *Proc. Natl. Acad. Sci. USA* **98**, 7158–7163.

Chan, J.Y., Han, X. & Kan, Y.W. (1993) Cloning of Nrf1, an NF-E2-related transcription factor, by genetic selection in yeast. *Proc. Natl. Acad. Sci. USA* **90**, 11371–11375.

Chidsey, C.E.D. & Loiacono, D.N. (1990) Chemical functionality in self-assembled monolayers: structural and electrochemical properties. *Langmuir* **6**, 682–691.

Dlakic, M., Grinberg, A.V., Leonard, D.A. & Kerppola, T.K. (2001) DNA sequence-dependent folding determines the divergence in binding specificities between Maf and other bZIP proteins. *EMBO J.* **20**, 828–840.

Fujiwara, K.T., Kataoka, K. & Nishizawa, M. (1993) Two new members of the *maf* oncogene family, *maf* K and *maf* F, encode nuclear b-Zip proteins lacking putative trans-activator domain. *Oncogene* **8**, 2371–2381.

Galio, L., Briquet, S., Cot, S., Guillet, J.G. & Vaquero, C. (1997) Analysis of interactions between huGATA-3 transcription factor and three GATA regulatory elements of HIV-1 long terminal repeat, by surface plasmon resonance. *Anal. Biochem.* **253**, 70–77.

George, A.J., French, R.R. & Glennie, M.J. (1995) Measurement of kinetic binding constants of a panel of anti-saporin antibodies using a resonant mirror biosensor. *J. Immunol. Methods* **183**, 51–63.

Huang, J., Dahlgren, D.A. & Hemminger, J.C. (1994) Photo-patterning of self-assembled alkanethiolate monolayers on gold: a simple monolayer photoresist utilizing aqueous chemistry. *Langmuir* **10**, 626–628.

Itoh, K., Chiba, T., Takahashi, S., *et al.* (1997) An Nrf2/small Maf heterodimer mediates the induction of phase II detoxifying enzyme genes through antioxidant response elements. *Biochem. Biophys. Res. Commun.* **236**, 313–322.

Itoh, K., Igarashi, K., Hayashi, N., Nishizawa, M. & Yamamoto, M. (1995) Cloning and characterization of a novel erythroid cell-derived CNC family transcription factor heterodimerizing with the small Maf family proteins. *Mol. Cell. Biol.* **15**, 4184–4193.

Jordan, C.E. & Corn, R.M. (1997) Surface plasmon resonance imaging measurements of electrostatic biopolymer adsorption onto chemically modified gold surfaces. *Anal. Chem.* **69**, 1449–1456.

Jost, J.P., Munch, O. & Andersson, T. (1991) Study of protein–DNA interactions by surface plasmon resonance (real time kinetics). *Nucl. Acids Res.* **19**, 2788.

Kataoka, K., Fujiwara, K.T., Noda, M. & Nishizawa, M. (1994a) MafB, a new Maf family transcription activator that can associate with Maf and Fos but not with Jun. *Mol. Cell. Biol.* **14**, 7581–7591.

Kataoka, K., Igarashi, K., Itoh, K., *et al.* (1995) Small Maf proteins heterodimerize with Fos and potentially act as competitive repressors of NF-E2 transcription factor. *Mol. Cell. Biol.* **15**, 2180–2190.

Kataoka, K., Noda, M. & Nishizawa, M. (1994b) Maf nuclear oncoprotein recognizes sequences related to an AP-1 site and forms heterodimers with both Fos and Jun. *Mol. Cell. Biol.* **14**, 700–712.

Katsuoka, F., Motohashi, H., Tamagawa, Y., *et al.* (2003) Small Maf compound mutants display central nervous system neuronal degeneration, aberrant transcription, and Bach protein mis-localization coincident with myoclonus and abnormal startle response. *Mol. Cell. Biol.* **23**, 1163–1174.

Kerppola, T.K. & Curran, T.A. (1994) A conserved region adjacent to the basic domain is required for recognition of an extended DNA binding site by Maf/Nrl family proteins. *Oncogene* **9**, 3149–3158.

Kobayashi, A., Ito, E., Toki, T., *et al.* (1999) Molecular cloning and functional characterization of a new Cap'n'collar family transcription factor Nrf3. *J. Biol. Chem.* **274**, 6443–6452.

Kumar, R., Chen, S., Scheurer, D., *et al.* (1996) The bZIP transcription factor Nrl stimulates rhodopsin promoter activity in primary retinal cell cultures. *J. Biol. Chem.* **271**, 29612–29618.

Kusunoki, H., Motohashi, H., Katsuoka, F., Morohashi, A., Yamamoto, M. & Tanaka, T. (2002) Solution structure of the DNA-binding domain of MafG. *Nature Struct. Biol.* **9**, 252–256.

MacBeath, G. & Schreiber, S.L. (2000) Printing proteins as microarrays for high-throughput function determination. *Science* **289**, 1760–1763.

Moi, P., Chan, K., Asunis, I., Cao, A. & Kan, Y.W. (1994) Isolation of NF-E2-related factor 2 (Nrf2), a NF-E2-like basic leucine zipper transcriptional activator that binds to the tandem NF-E2/AP1 repeat of the beta-globin locus control region. *Proc. Natl. Acad. Sci. USA* **91**, 9926–9930.

Motohashi, H., Katsuoka, F., Shavit, J.A., Engel, J.D. & Yamamoto, M. (2000) Positive or negative MARE-dependent transcriptional regulation is determined by the abundance of small Maf proteins. *Cell* **103**, 865–875.

Motohashi, H., O'Connor, T., Katsuoka, F., Engel, J.D. & Yamamoto, M. (2002) Integration and diversity of the

regulatory network composed of Maf and CNC families of transcription factors. *Gene* **294**, 1–12.

Nelson, B.P., Frutos, A.G., Brockman, J.M. & Corn, R.M. (1999) Near-infrared surface plasmon resonance measurements of ultrathin films. 1. Angle shift and SPR imaging experiments. *Anal. Chem.* **71**, 3928–3934.

Newman, J.R. & Keating, A.E. (2003) Comprehensive identification of human bZIP interactions with coiled-coil arrays. *Science* **300**, 2097–2101.

Nishizawa, M., Kataoka, K., Goto, N., Fujiwara, K.T. & Kawai, S. (1989) v-maf, a viral oncogene that encodes a 'leucine zipper' motif. *Proc. Natl. Acad. Sci. USA* **86**, 7711–7715.

Oda, M., Furukawa, K., Sarai, A. & Nakamura, H. (1999) Kinetic analysis of DNA binding by the c-Myb DNA-binding domain using surface plasmon resonance. *FEBS Lett.* **454**, 288–292.

Ogino, H. & Yasuda, K. (1998) Induction of lens differentiation by activation of a bZIP transcription factor, L-Maf. *Science* **280**, 115–118.

Oyake, T., Itoh, K., Motohashi, H., *et al.* (1996) Bach proteins belong to a novel family of BTB-basic leucine zipper transcription factors that interact with MafK and regulate transcription through the NF-E2 site. *Mol. Cell. Biol.* **16**, 6083–6095.

Schena, M., Shalon, D., Davis, R.W. & Brown, P.O. (1995) Quantitative monitoring of gene expression patterns with a cDNA microarray. *Science* **270**, 467–470.

Seimiya, M. & Kurosawa, Y. (1996) Kinetics of binding of Antp homeodomain to DNA analyzed by measurements of surface plasmon resonance. *FEBS Lett.* **398**, 279–284.

Stamatoyannopoulos, J.A., Goodwin, A., Joyce, T. & Lowrey, C.H. (1995) NF-E2 and GATA binding motifs are required for the formation of DNase I hypersensitive site 4 of the human beta-globin locus control region. *EMBO J.* **14**, 106–116.

Sun, J., Hoshino, H., Takaku, K., *et al.* (2002) Hemoprotein Bach1 regulates enhancer availability of heme oxygenase-1 gene. *EMBO J.* **21**, 5216–5224.

Suzuki, F., Goto, M., Sawa, C., *et al.* (1998) Functional interaction of transcription factor human GA-binding protein subunits. *J. Biol. Chem.* **273**, 29302–29308.

Swaroop, A., Xu, J., Pawer, H., Jackson, A., Scolnick, C. & Agarwal, N. (1992) A conserved retina-specific gene encodes a basic motif/leucine zipper protein. *Proc. Natl. Acad. Sci. USA* **89**, 266–270.

Tanikawa, J., Yasukawa, T., Enari, M., *et al.* (1993) Recognition of specific DNA sequences by the c-myb protooncogene product: role of three repeat units in the DNA-binding domain. *Proc. Natl. Acad. Sci. USA* **90**, 9320–9324.

Tarlov, M.J., Burgess, D.R.F. & Gillen, J.G. (1993) UV photo-patterning of alkanethiolate monolayers self-assembled on gold and silver. *J. Am. Chem. Soc.* **115**, 5305–5306.

Troughton, E.B., Bain, C.D., Whitesides, G.M., Nuzzo, R.G., Allara, D.L. & Porter, M.D. (1988) Monolayer films prepared by the spontaneous self-assembly of symmetrical and un-symmetrical dialkyl sulfides from solution onto gold substrates: structure, properties, and reactivity of constituent functional groups. *Langmuir* **4**, 365–385.

Venugopal, R. & Jaiswal, A.K. (1996) Nrf1 and Nrf2 positively and c-Fos and Fra1 negatively regulate the human antioxidant response element-mediated expression of NAD (P) H: quinone oxidoreductase1 gene. *Proc. Natl. Acad. Sci. USA* **93**, 14960–14965.

Yamamoto, M., Ko, L.J., Leonard, M.W., Beug, H., Orkin, S.H. & Engel, J.D. (1990) Activity and tissue-specific expression of the transcription factor NF-E1 [GATA] multigene family. *Genes Dev.* **4**, 1650–1662.

Zhu, H., Bilgin, M., Bangham, R., *et al.* (2001) Global analysis of protein activities using proteome chips. *Science* **293**, 2101–2105.